A NON QUASI-STATIC NON-LINEAR P-HEMT MODEL OPERATING UP TO MILLIMETRIC FREQUENCIES

Daniel Roques, Francis Brasseau, Bernard Cogo, Michel Soulard, Jean-Louis Cazaux

ALCATEL SPACE INDUSTRIES, 26, Avenue J.F. Champollion, B.P. 1187

31037 Toulouse Cedex- FRANCE

Tel : 33.5.34.35.58.41 - Fax : 33.5.34.35.69.47-E-mail : daniel.roques.@space.alcatel.fr

ABSTRACT

This paper presents a non-linear p-HEMT model taking into account the non quasi-static currents and charges variations versus Vgs and Vds to predict accurate behaviour of the devices up to millimetric frequencies. The major refinement of this model concerns the introduction of voltage dependant 2nd order frequency coeficients (1st order non quasi-static terms) generally considered constant or partially variable in previous published models. The non quasi-static behaviour of the transistor is modelled by time second derivatives of non-linear functions Ags(vgs,vds) and Ads(vgs,vds) integrated from linear 2nd order frequency coefficients. Classical method are used to extract non-linear elements from pulsed S-parameters and current measurement set-up [1]. Most of the voltage dependant coefficients (currents, charges and non-quasi-static terms) are precisely fitted with bicubic spline functions for very accurate description. This model has been implemented in commercial balance harmonic software. Ags and Ads time second derivatives are generated partially in the non-linear part of the model (time first derivative considered as charge derivative) and partially with a linear sub-circuit (second derivative). This model would predict more accurate 2nd and 3rd harmonics behaviour for applications at fundamental frequencies up to 20 GHz.

INTRODUCTION

The emergence of advanced microwave devices for high frequency applications (up to Ka band) such as power p-HEMT, has been followed by the development of associated millimetric circuits. However, the success in the design of these circuits depends critically on the accuracy of the device models in high non-linear and high frequency conditions. In the past years, important works have been performed to overcome the limitations presented by the classical FET models based on lumped elements topology. New topologies taking into account the distribution nature of the channel under the gate have been published [2] [3] with interesting results.
The aim of our work was to develop a model based on physical consideration (distributed effects) describing with accuracy the non-linear and 1st order non-quasi-static behaviour to be implemented in commercial software (Libra Harmonic balance software from HP-EESOF™) and able to predict 2nd and 3rd harmonic behaviour for applications up to 20 GHz fundamental frequencies.

LINEAR MODEL DERIVATION

The physical behaviour of the p-HEMT intrinsic region can be modelled in small signal conditions by a distributed non-uniform R-C-gm network (figure 1) whose representative differential equation versus x (position along channel length) is as follows :

$$\frac{\partial^2 v(x,\omega)}{\partial x^2} = (jRC\omega + R\frac{dgm}{dx})v + (\frac{1}{R}\frac{dR}{dx} + Rgm)\frac{\partial v(x,\omega)}{\partial x} \quad (1)$$

It could be demonstrated that from resolution of equation (1) we can derive Y parameters with following form :

$$Y_{ij} = \sum_{k=0}^{\infty} (j\omega)^k . a_{ijk} \quad (2)$$

The second order approximation of Y parameters expression is written :

$$Y_{ij} = a_{ij0} + j\omega a_{ij1} - \omega^2 a_{ij2} \quad (3)$$

The coefficients a_{ij0} and a_{ij1} can be respectively identified with a conductance g_{ij} and a capacitance C_{ij} . The second order term represents the non quasi-static behaviour (coefficient a_{ij2} replaced here after by - α_{ij}). In these conditions , the second order approximation of Y_{ij} can be written:

$$Y_{ij} = g_{ij} + j\omega C_{ij} + \omega^2 \alpha_{ij} \quad (4)$$

From S parameters measurements, a very easy and direct extraction method may be applied to extract g_{ij} , C_{ij} and α_{ij} . The terms C_{ij} are obtained from imaginary part of Y_{ij} :

$$C_{ij} = \frac{Im(Y_{ij})}{\omega} \tag{5}$$

and g_{ij} and α_{ij} are extracted by a least square method (1^{st} order) applied to real part of Y_{ij} : $Re(Y_{ij}) = g_{ij} + \omega^2 \alpha_{ij}$ ($g_{ij} = Re(Y_{ij})$ for $X = \omega^2 = 0$ and α_{ij} = slope of $Re(Y_{ij})$ versus $X = \omega^2$)

NON-LINEAR MODEL

The non-linear current I_{drain} flowing from drain port is integrated from small-signal expression as follows :

$$dI_{drain} = Y_{21} .dvgS + Y_{22} .dvds \tag{6}$$

So, $$dI_{drain} = g_{21}dvgs + g_{22}dvds + j\omega(C_{21}dvgs + C_{22}dvds) + \omega^2(\alpha_{21}dvgs + \alpha_{22}dvds) \tag{7}$$

We assume α_{21} and α_{22} as partial derivatives of a Ads function respectively versus Vgs and Vds .

So, $$dI_{drain} = dIds + \frac{d}{dt}(dQds) + \frac{d^2}{dt^2}(dAds) \tag{8}$$

and by integration versus vgs and vds :

$$I_{drain} = \int_{vgs,vds} d1_{drain} = \int_{vgs,vds} dIds + \int_{vgs,vds} (\frac{d}{dt}Qds) + \int_{vgs,vds} \frac{d^2}{dt^2}(dAds) \tag{9}$$

The integration versus vgs and vds being time independent ,

$$I_{drain} = \int_{vgs,vds} dIds + \frac{d}{dt}(\int_{vgs.vds} dQds) + \frac{d^2}{dt^2}(\int_{vgs,vds} dAds) = Ids + \frac{dQds}{dt} + \frac{d^2Ads}{dt2} \tag{10}$$

The same approach is applied to compute the current flowing from gate port ($I_{gate} = Igs + \frac{dQgs}{dt} + \frac{d^2Ags}{dt^2}$).

The non-linear model topology is presented on figure 2. Qgs and Qds charges are obtained by integration of measured C_{ij} and Ags and Ads functions by integration of measured α_{ij}. The non-linear currents sources Igs and Ids are extracted from pulsed currents measurements. Ids current generator ,Qgs and Qds charges and non-quasic static functions Ads and Ads are fitted by bicubic spline functions. The time second derivative of Ags and Ads are generated in the software partially in the non-linear part of the model (time first derivative considered as charge derivative) and partially with a linear sub-circuit (second derivative) (figure 3). The non-linear model of a lmm p-HEMT (0.25 µm gate length) has been extracted from S-parameters measurements performed up to 17 GHz. Modelling/measurements comparison for the non-linear elements are presented on figures 4 to 16. Major discrepancies are observed for α_{22} parameter in the saturated region. The reason is the unprecise extraction of this parameter due to high relative value of the output conductance g_{22} (extracted values of are aberrant and not represented on figure 16). More accurate α_{ij} could be obtained from higher frequency measurements (up to 40 GHz [1]).

CONCLUSION

A non-linear p-HEMT model taking into account 1^{st} order non-quasi-static effects has been presented. This model is implementable in commercial balance harmonic software. The accurate description of voltage dependant frequency second order terms would improve prediction of significant harmonics for application frequencies up to 20 GHz.

REFERENCES

[l] J.P. Teyssier et al " Fully integrated non-linear modelling and characterization system of microwave transistors with on-wafer measurements", in IEEE MMT-S Symp., Orlando, FL, 1995, pp. 1033-1036

[2] B. Mallet-Guy et al, " A distributed , measurements based, non linear model of FET's for high frequency applications", IEEE-MTT Symposium digest, Denver, CO, 1997, pp.869-872.

[3] Robert R. Daniels et al, " A Universal Large/Small Signal 3-Terminal FET Model Using a Non Quasi-Static Charged-Based Approach ", IEEE Trans. on Electron Devices, Vol 40, N°10, October 1993, pp. 1723-1729.

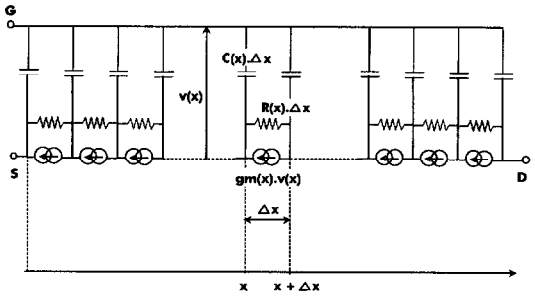

Figure 1 : non-uniform R-C-gm network

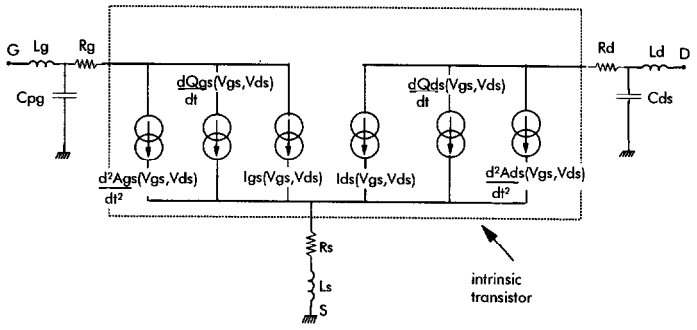

Figure 2 : Non-linear model

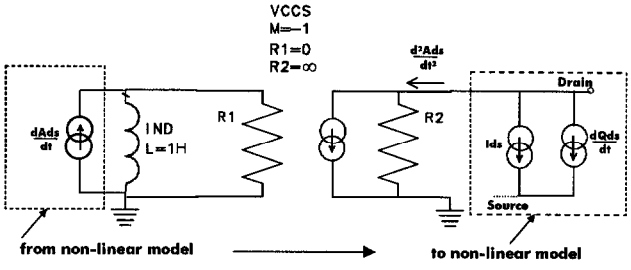

VCCS = Voltage controlled current source
M = transconductance

Figure 3 : $\frac{dAds}{dt}$ time derivative linear sub-circuit

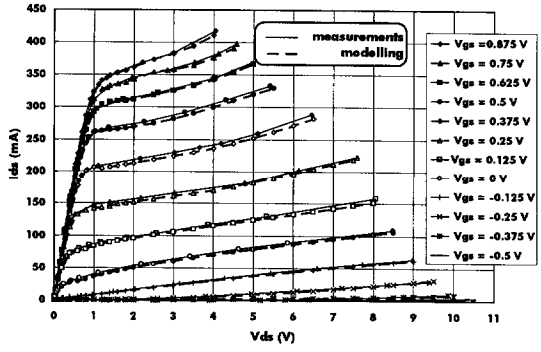

Figure 4 : measured and modelled Ids current

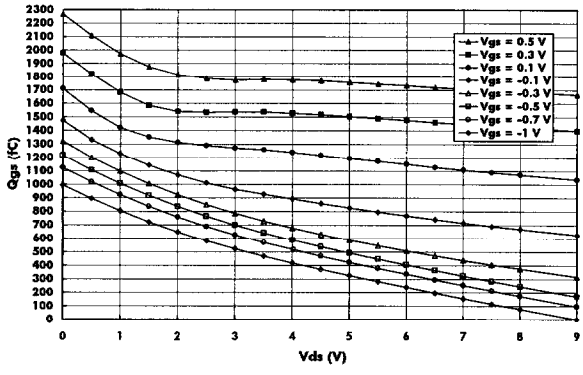

Figure 5 : Qgs (integrated from measured C11 and C12)

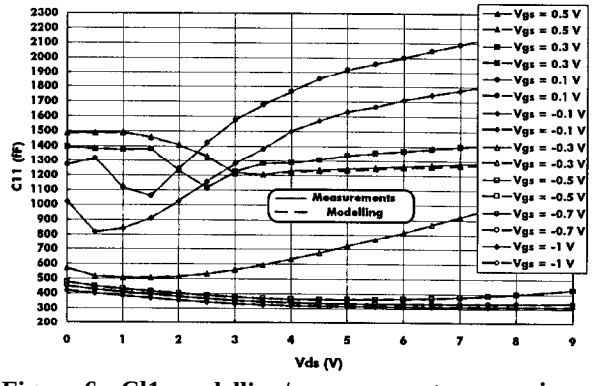

Figure 6 : Cl1 modelling/measurement comparison

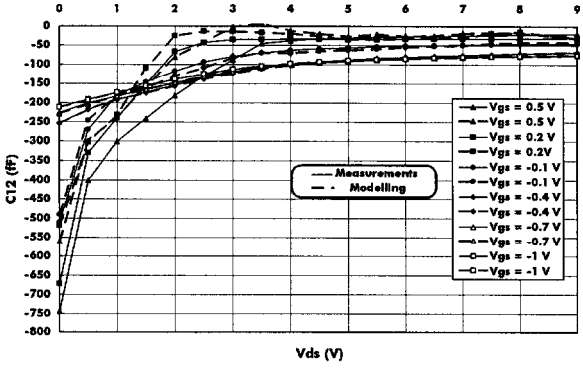

Figure 7 : Cl2 modelling/measurement comparison

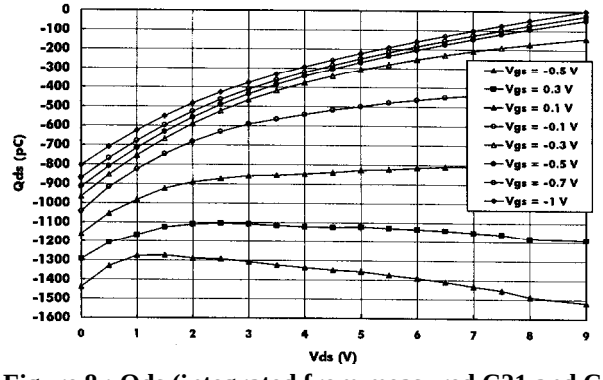

Figure 8 : Qds (integrated from measured C21 and C22)

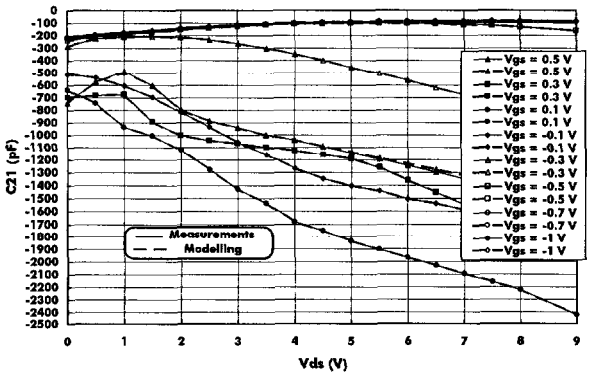

Figure 9 : C21 modelling/measurement comparison

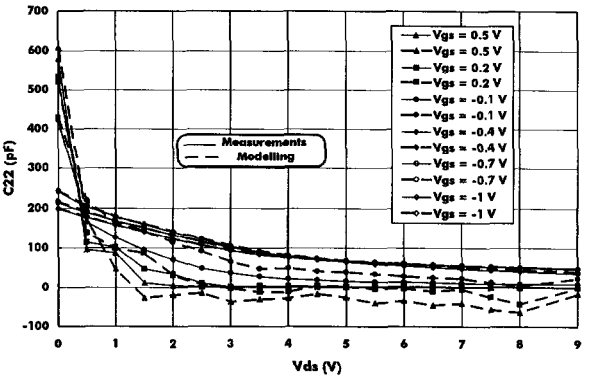

Figure 10 : C22 modelling/measurement comparison

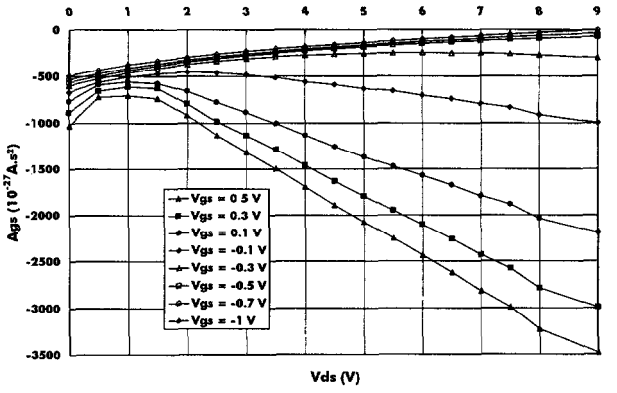

Figure 11 : Ags (integrated from measured α11 and α12)

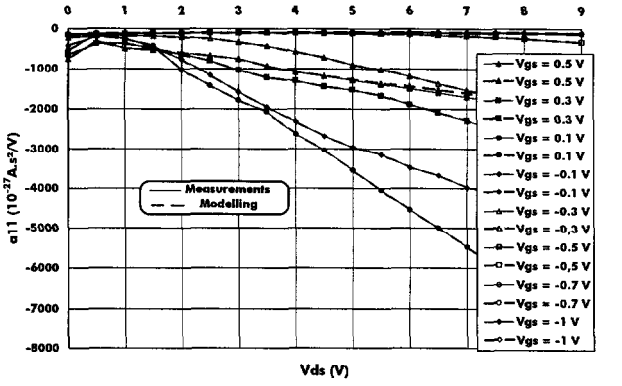

Figure 12 : α11 modelling/measurement comparison

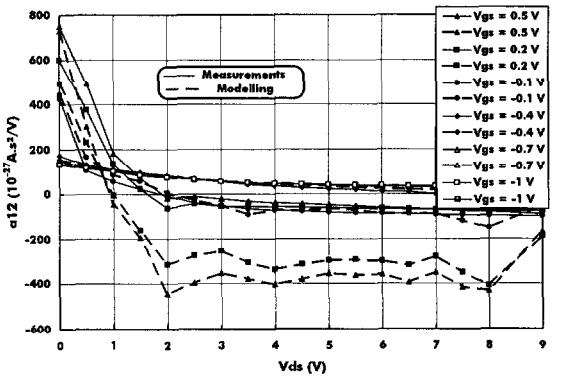

Figure 13 : α12 modelling/measurement comparison

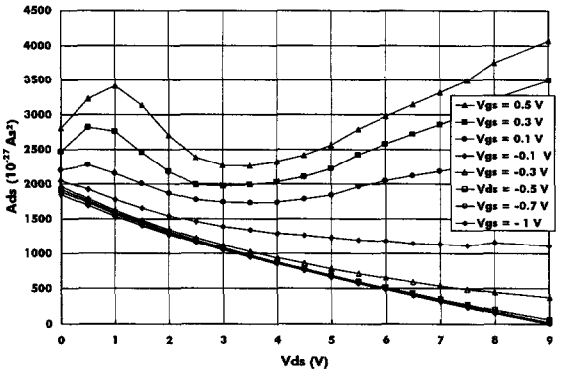

Figure 14 : Ads (integrated from meas. α21 and α22)

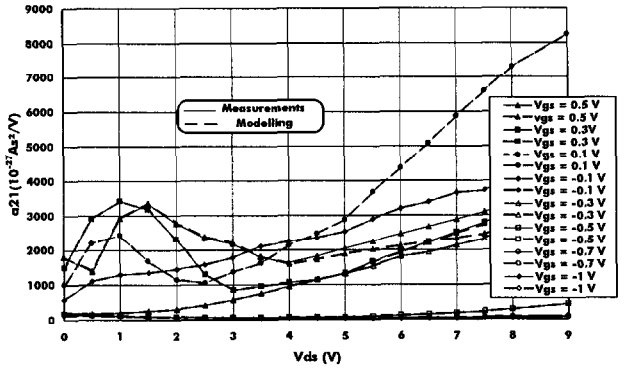

Figure 15 : α21 modelling/measurement comparison

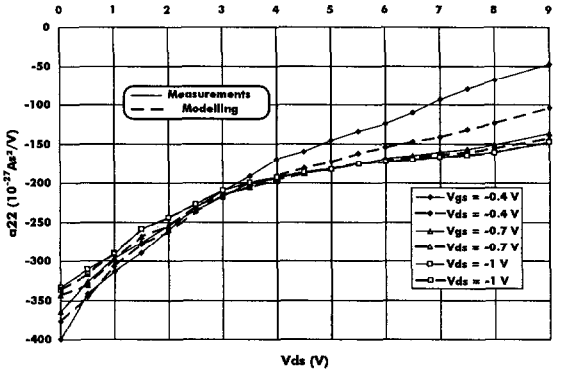

Figure 16 : α22 modelling/measurement comparison